

Spin-glass dynamics of $\text{La}_{0.95}\text{Sr}_{0.05}\text{CoO}_3$

D. N. H. Nam

*Department of Materials Science, Uppsala University, Box 534, S-751 21 Uppsala, Sweden
and Institute of Materials Science, NCST, Nghiado-Caugiay-Hanoi, Vietnam*

R. Mathieu and P. Nordblad

Department of Materials Science, Uppsala University, Box 534, S-751 21 Uppsala, Sweden

N. V. Khiem

Department of Science and Technology, Hongduc University, Thanhhoa, Vietnam

N. X. Phuc

Institute of Materials Science, NCST, Nghiado-Caugiay-Hanoi, Vietnam

(Received 5 May 2000)

Experimental studies of dynamic magnetic properties of a highly homogeneous sample of $\text{La}_{0.95}\text{Sr}_{0.05}\text{CoO}_3$ perovskite evidence the existence of a low-temperature spin-glass phase. A dynamic scaling analysis of ac susceptibility data according to conventional critical slowing down implies a finite spin-glass phase-transition temperature $T_g \approx 14.6$ K and a dynamic exponent $z\nu \approx 10.3$. Low-field magnetic relaxation experiments show essentially logarithmic magnetic relaxation and aging effects at all temperatures below T_g and that temperature perturbations affect the relaxation function in a way that is characteristic for a low-temperature spin-glass phase. Finally, it is also shown that “simple” remanent magnetization vs temperature curves, measured after specific cooling protocols, can yield information on dynamic properties such as aging and memory phenomena.

I. INTRODUCTION

Although the $\text{La}_{1-x}\text{Sr}_x\text{CoO}_3$ (LSCO) compounds do not show a colossal magnetoresistance as do their manganese $\text{La}_{1-x}\text{Sr}_x\text{MnO}_3$ counterparts, their magnetic behavior is very intriguing. In a pioneering work, Itoh *et al.*¹ presented a phase diagram for the LSCO system where there exists a sharp change of the magnetic properties at $x=0.18$; the $0.18 \leq x \leq 0.5$ region is named “cluster glass” and a spin-glass (SG) phase is assigned to $0 < x < 0.18$.

For the region $x \geq 0.18$, as reported in several previous studies,^{2,3} glassy behavior is seen in compounds with $x = 0.5$, which can be considered as a typical high Sr-content compound of the “cluster-glass” phase. In a recent study of an $x=0.3$ sample by Caciuffo *et al.*,⁴ neutron diffraction and small-angle neutron scattering showed that short-range ferromagnetic correlation persists also at temperatures well above T_c . Both the number and sizes of the clusters slightly increase with decreasing temperature but suddenly decrease as the temperature goes through T_c . Concurrent neutron-diffraction results by Caciuffo *et al.*⁵ evidence the existence of ferromagnetic clusters with short-range correlations in all LSCO compounds with $0.1 \leq x \leq 0.3$. However, in another neutron-diffraction study by Sathe *et al.*,⁶ ferromagnetic ordering was only observed for $x \geq 0.2$. A concurring result from neutron-scattering studies is that antiferromagnetic correlations are never observed.⁴⁻⁷

In the proclaimed spin-glass region, dynamic scaling analyses on an $x=0.15$ sample have recently revealed that there is no true SG phase at finite temperatures, although glassy dynamics is observed.⁸ A neutron-scattering study on a $\text{La}_{0.92}\text{Sr}_{0.08}\text{CoO}_3$ single crystal showed that the paramag-

netic scattering increases steadily with decreasing temperature until a leveling off is observed below $T_f=24$ K, the same temperature as that where a freezing of the magnetic moments is observed in magnetization measurement.⁷ This observation suggests that the sample enters a spin-glass phase at low temperatures. Nevertheless, short-range ferromagnetic correlation was still observed at all measuring temperatures below T_f and also up to temperatures as high as 600 K; the derived correlation length is about 8 Å and does not change significantly with temperature, even when passing through T_f . The authors suggested that the spin-glass behavior could be caused by long-range Ruderman-Kittel-Kasuya-Yosida type interaction between the magnetic clusters. In addition, it has recently been proposed that in all LSCO compounds there is a formation of polarons—which might correspond to magnetic clusters—originating from local Jahn-Teller distortions.⁹

Contradictory results on the magnetic properties of LSCO samples of similar nominal composition have been reported by different research groups. This fact reflects the difficulties related to fabricating high-quality LSCO materials, e.g., it seems exceedingly difficult to obtain a fully homogeneous distribution of Sr^{2+} ions. Several magnetic properties of the LSCO system are thus still not unambiguously settled. This is especially true for the low Sr-concentration compounds where the magnetic properties of the stoichiometric phase may be masked by “ferromagnetic cluster” effects arising from an inhomogeneous distribution of the Sr^{2+} ions.

One of the remaining open questions for the LSCO system is whether there exists a true spin-glass phase or not at low Sr concentrations. We have fabricated a high-quality $\text{La}_{0.95}\text{Sr}_{0.05}\text{CoO}_3$ sample and investigated its magnetic dy-

namics by ac susceptibility, dc magnetization and time-dependent magnetic relaxation experiments. The results give strong evidence for the existence of a low-temperature spin-glass phase.

II. EXPERIMENTS

The $\text{La}_{0.95}\text{Sr}_{0.05}\text{CoO}_3$ compound was prepared by the standard solid-state reaction method. Stoichiometric amounts of La_2O_3 , SrCO_3 , and Co_3O_4 were carefully mixed in ethanol. The dried powder was pressed into pellets and calcined at 1423 K in air for two months with several intermediate grindings. Afterwards, the calcinated pellets were sintered at 1623 K for 12 h and then slowly cooled down to room temperature. The final product was examined by x-ray diffraction technique showing a single phase material of rhombohedral structure.

The temperature dependence of the zero-field-cooled (ZFC), field-cooled (FC), thermo-remnant (TRM), and isothermal remnant (IRM) magnetization was measured using a Quantum Design MPMS5 superconducting quantum interference device (SQUID) magnetometer. In the ZFC measurements the sample was cooled from room temperature to 5 K in zero field before the application of the magnetic field. For the FC and TRM measurements the sample was cooled in an applied field to 5 K, which was switched off at 5 K for the TRM measurements. The $M_{\text{ZFC}}(T)$, $M_{\text{FC}}(T)$, $M_{\text{TRM}}(T)$, and $M_{\text{IRM}}(T)$ data were all recorded during reheating. A Lakeshore 7225 susceptometer was used for the ac-susceptibility measurements at the frequencies $\omega/2\pi = 15, 125, \text{ and } 1000$ Hz. Low-frequency data ($\omega/2\pi = 51, 5.1, 1, 0.51, 0.1, \text{ and } 0.051$ Hz) were measured using a Cryogenic S600 SQUID susceptometer. Relaxation of ZFC magnetization $m(t)$ and temperature cycling experiments were made in a noncommercial low-field SQUID system.¹⁰ In these experiments, the sample was cooled in zero field from a reference temperature of 270 K to a measuring temperature T_m and kept there a wait time t_w before the application of a small probing field h . $m(t)$ was then recorded as a function of the time elapsed after the field application. In the temperature cycling experiments,¹¹ the sample was additionally subjected to a temperature cycle ΔT just after the wait time and immediately prior to the application of the magnetic field.

The field-cooling history dependence of the remanent magnetization was investigated using special experimental procedures that will be described below.

III. RESULTS AND DISCUSSION

A. dc magnetization and ac susceptibility

The main frame of Fig. 1 shows the temperature dependence of $M_{\text{ZFC}}(T)$ and $M_{\text{FC}}(T)$ in an applied field of 20 Oe. $M_{\text{ZFC}}(T)$ exhibits a cusp at about 15 K and coalesces with $M_{\text{FC}}(T)$ at a slightly higher temperature. These features of the dc-magnetization are also the most simple signatures of a conventional spin glass. It is worth noting that for this LSCO sample $M_{\text{ZFC}}(T)$ and $M_{\text{FC}}(T)$ coalesce just above the cusp in the ZFC curve, an indication that the sample has a highly homogeneous distribution of Sr^{2+} ions.

The inset of Fig. 1 shows the in-phase component of the ac-susceptibility vs temperature at three different frequen-

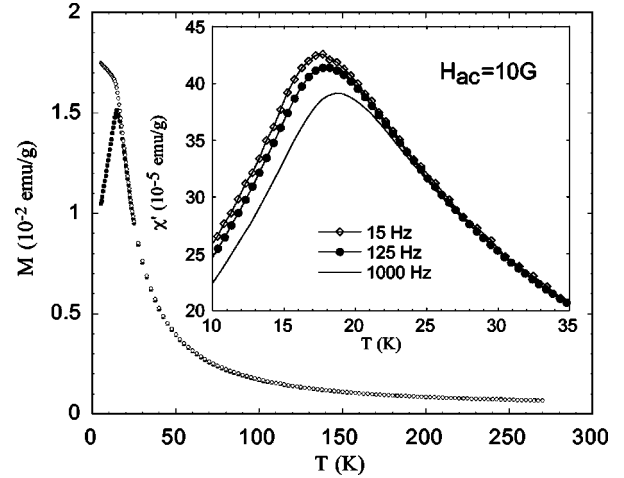


FIG. 1. M_{ZFC} and M_{FC} vs temperature using an applied field of 20 Oe. The inset shows $\chi'(T)$ using an ac field of 10 Oe at different frequencies 15, 125, and 1000 Hz. All data were measured on heating.

cies. $\chi'(T)$ attains a maximum at T_f that shifts towards higher temperatures with higher frequencies. Below the maximum, the magnitude of χ' is frequency dependent, but it becomes independent of frequency at temperatures just above T_f . This behavior is qualitatively similar to that of a conventional spin glass. With decreasing temperature from the paramagnetic state the relaxation time of the spin glass slows down leading to a divergence of the maximum relaxation time at T_g , where the system enters the spin-glass state. The frequency-dependent maximum in χ' indicates the freezing temperature T_f where the maximum relaxation time, τ , of the system is equal to the characteristic time $t = 1/\omega$ set by the frequency of the ac-susceptibility measurement. By measuring the variation of T_f in a wide range of frequencies we can judge if a spin glass phase is approached by a fit of the data to conventional critical slowing down,¹²

$$\frac{\tau}{\tau_0} \propto \left(\frac{T_f - T_g}{T_g} \right)^{-z\nu}.$$

The best fit, which is displayed in Fig. 2, uses $T_g \approx 14.6$ K, $z\nu \approx 10.3$ and $\tau_0 \approx 2.3 \times 10^{-10}$ s. The obtained magnitude of τ_0 is larger than in conventional spin glasses ($\tau_0 \approx 10^{-13}$ s). It is however still of reasonable size, since the microscopic magnetic entities in LSCO probably are not single atomic spins, but nano-sized clusters of ferromagnetically coupled spins. The value of $z\nu$ is consistent with that of conventional three-dimensional (3D) spin glasses.¹³

B. Relaxation and aging

The relaxation time of a spin glass diverges at T_g , and remains infinite also at lower temperatures. In this temperature region, the spin glass exhibits slow logarithmic relaxation on all time scales as well as aging phenomena.¹⁴ The time dependence of the zero-field-cooled magnetization, $m(t)$, of $\text{La}_{0.95}\text{Sr}_{0.05}\text{CoO}_3$ measured in the spin-glass phase is plotted vs $\log t$ in Fig. 3(a). In the relaxation measurements depicted in this figure, the system was kept at $T_m = 10$ K for different wait times, $t_w = 10^2, 10^3$ and 10^4 s, in zero field

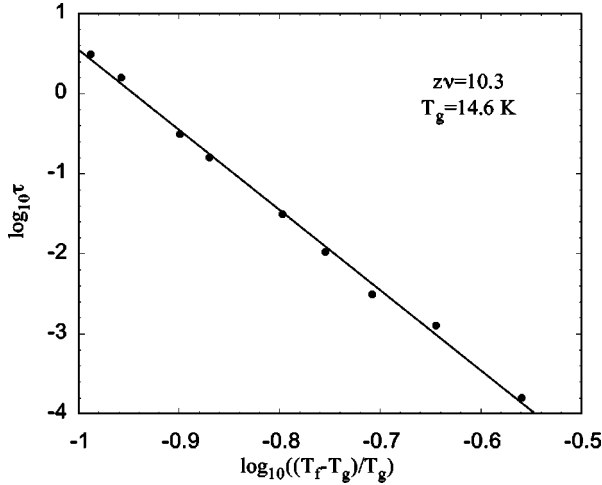


FIG. 2. The best fit of $T_f(\omega)$ data extracted from ac susceptibility measurements to $\tau/\tau_0 = [(T_f - T_g)/T_g]^{-z\nu}$. $T_g = 14.6$ K and $z\nu = 10.3$.

before the magnetization was recorded as a function of time elapsed after the field application. The shape of the $m(t)$ curves changes with changing t_w , implying an age-dependent phenomenon. The most striking feature being that all the $m(t)$ curves have an inflection point at an observation time closely equal to t_w . In Fig. 3(b) the corresponding relaxation rates, $S(t) = 1/h(\partial m(t)/\partial \log_{10} t)$, are plotted vs $\log_{10} t$. The curves show a maximum at the observation time where the inflection point is observed in the corresponding $m(t)$ curves. A similar aging behavior is observed at other finite temperatures below T_g .

One early theoretical approach that predicts aging effects in spin glasses is the droplet model¹⁵ in which the maximum of the relaxation rate can be interpreted to be associated with a crossover from quasiequilibrium dynamics at short observation times ($t \ll t_w$) to nonequilibrium dynamics at long observation times ($t \gg t_w$). Aging phenomena in glassy systems are currently subject to intense theoretical work.¹⁶ Results from Monte Carlo simulations for two- and three-dimensional Ising spin-glass systems show that the relaxation rate $S(t)$ indeed exhibits a maximum at $t \approx t_w$.¹⁷ However, nonequilibrium dynamic effects in the magnetic relaxation very similar to those reported here for $\text{La}_{0.95}\text{Sr}_{0.05}\text{CoO}_3$, have also been observed in a variety of disordered and frustrated systems including some mixed valent perovskites (R,A)MO₃ such as $\text{La}_{0.85}\text{Sr}_{0.15}\text{CoO}_3$,⁸ $\text{La}_{0.5}\text{Sr}_{0.5}\text{CoO}_3$,^{2,18} $\text{Nd}_{0.7}\text{Sr}_{0.3}\text{MnO}_3$,¹⁹ and $\text{Y}_{0.7}\text{Ca}_{0.3}\text{MnO}_3$.²⁰

Low fields are required to probe intrinsic nonequilibrium dynamics of frustrated and disordered magnets. A too strong field will disturb the equilibration process and modify the dynamics. However, under a sufficiently low field the system yields a linear response indicating that the field does not affect the intrinsic dynamics of the spin glass. An examination of field dependence of the response of our sample at 10 K is presented in the inset of Fig. 3(b). The five $S(t)$ curves measured in 10, 15, 20, 25, and 30 Oe all virtually merge into one line, i.e., a linear response is observed at least in fields up to 30 Oe for this temperature. Compared to many other disordered and frustrated systems, the dynamics of $\text{La}_{0.95}\text{Sr}_{0.05}\text{CoO}_3$ appears to be rather robust to magnetic fields. The CMR ferromagnet $\text{Nd}_{0.7}\text{Sr}_{0.3}\text{MnO}_3$ does not show

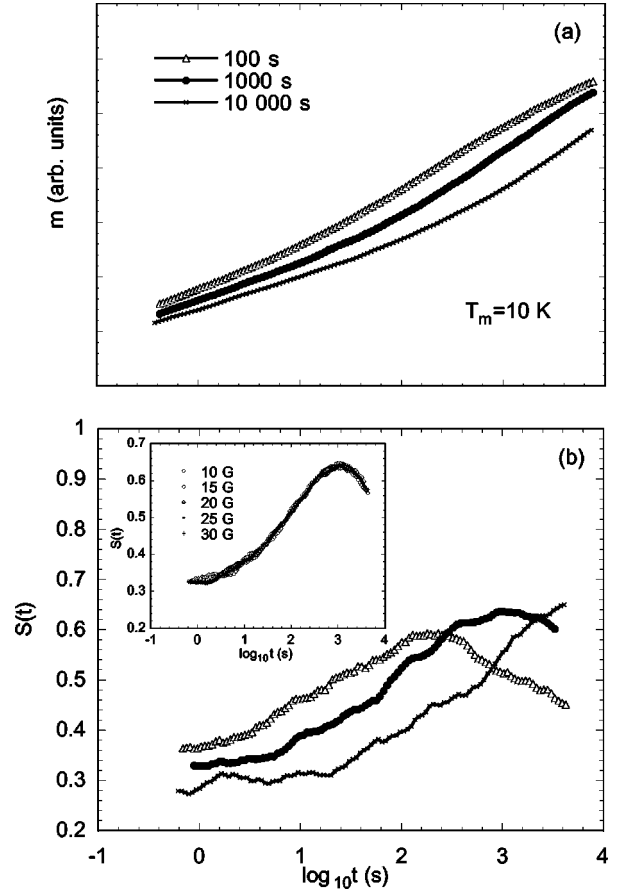


FIG. 3. (a) Relaxation of the ZFC magnetization, $m(t)$ vs $\log_{10} t$ and (b) the corresponding relaxation rate $S(t)$ vs $\log_{10} t$ recorded at $T_m = 10$ K in a field of $h = 10$ Oe after different wait times $t_w = 10^2, 10^3, \text{ and } 10^4$ s in zero field. The inset shows the relaxation rate measured in 10, 15, 20, 25, and 30 Oe, respectively; $t_w = 10^3$ s.

linear response even in fields as low as 0.2 Oe and observable aging is erased in fields above 2 Oe.¹⁹ Studies on a re-entrant ferromagnet²¹ show that the dynamics is more fragile in the ferromagnetic phase than in the spin-glass phase. The rather high fields up to which our sample shows linear response may be considered as indicative for a spin glass phase, but it is also a consequence of a rather low susceptibility of the sample.

Results from temperature cycling experiments can be used to distinguish SG states^{22,23} from other aging magnetic systems. Temperature cycling experiments on spin glasses have shown that an aging state established at T_m during a wait time at constant temperature is fully re-initialized by a large enough positive temperature cycle ΔT , but remains unaffected by a negative temperature cycle ΔT . I.e., the relaxation rate curve measured without a temperature cycle and the one with a negative temperature cycle of short duration are indistinguishable from each other, both showing a pronounced maximum at an observation time closely equal to t_w . A relaxation curve measured after a large enough positive temperature cycle however becomes fully reinitialized and similar to the relaxation curve measured immediately on reaching T_m after cooling from a temperature above T_g . Studies on a re-entrant ferromagnet²³ show that in the re-

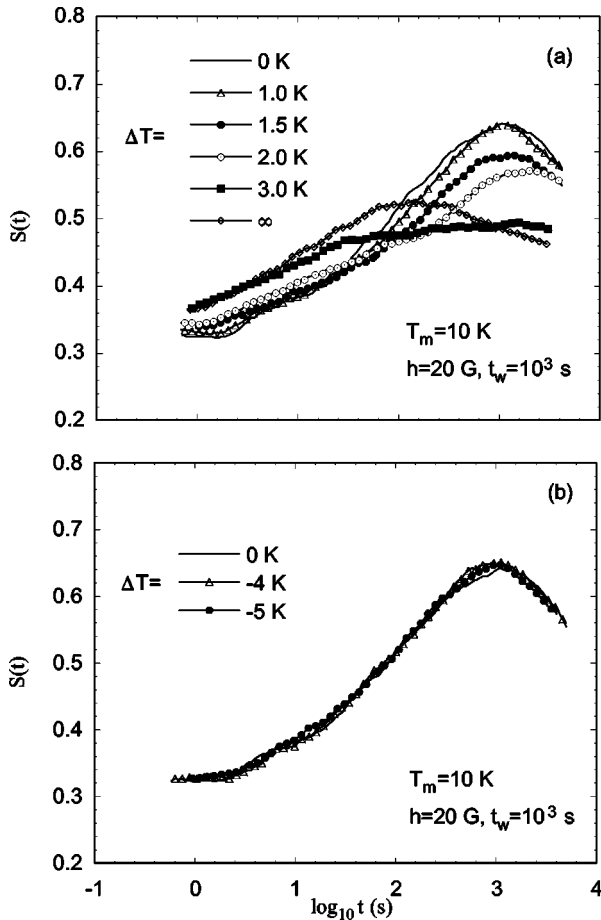


FIG. 4. $S(t)$ recorded at $T_m = 10$ K after positive (a) and negative (b) temperature cycles. A field of 20 Oe and a wait time of 10^3 s are used for all the measurements. Cycling temperatures $T_m + \Delta T$: (a) Positive temperature cycles: $\Delta T = 0, 1.0, 1.5, 2.0,$ and 3 K. The curve marked $\Delta T = \infty$ is $S(t)$ measured after a positive cycle which heats the system above T_g . (b) Negative temperature cycles: $\Delta T = 0, -4,$ and -5 K. The relaxation rate appears unaffected by the negative ΔT 's.

entrant spin-glass phase the behavior is similar to a conventional spin glass, while reinitialization occurs in the ferromagnetic phase irrespective of the sign of ΔT . A similar non-SG like behavior has also been seen in frustrated and disordered ferromagnets, i.e. the systems are reinitialized for both positive and negative temperature cyclings, ΔT .^{18,19} The temperature cycling results for $\text{La}_{0.95}\text{Sr}_{0.05}\text{CoO}_3$ displayed in Fig. 4 show characteristics of a conventional spin glass. In these experiments, the sample was aged for $t_w = 10^3$ s in zero field at $T_m = 10$ K before it was subjected to a temperature cycling $T_m + \Delta T$. When T_m was recovered, a probing field of 20 Oe was applied and the relaxation of the magnetization was recorded. The $\Delta T = \infty$ curve corresponds to $S(t)$ with $t_w = 0$ and shows a maximum at an observation time related to the ‘‘effective wait time’’ governed by the cooling rate and the time needed for thermal stabilization when approaching T_m . It is seen from the figure that for positive temperature cycles $\Delta T > 0$ of increasing magnitude, the original aging maximum of $S(t)$ at $t \approx 10^3$ s is suppressed and a new maximum appears at a short observation time, while for $\Delta T < 0$ [Fig. 4(b)] all measured $S(t)$ curves are closely identical implying that the aging states remain virtu-

ally unaffected by the temperature cycle, independent of its magnitude. I.e., a behavior characteristic to a spin-glass phase is observed.

It should be noted in this connection that the FC magnetization becomes cooling-rate dependent at temperatures close to T_g and below. Consequently, the FC magnetization also relaxes if the temperature is kept constant in this temperature range. This relaxation of our $\text{La}_{0.95}\text{Sr}_{0.05}\text{CoO}_3$ sample shows the characteristics of the relaxation of the field-cooled magnetization of an ordinary spin-glass phase:^{24–27} a downward relaxation of the field-cooled magnetization $M_{\text{FC}}(t)$ is observed well below T_g whereas only an upward relaxation is seen close to and slightly above T_g .

C. Temperature memory effect

The fact that a negative temperature cycling does not affect the aging at the higher temperature is the simplest example of a ‘‘memory effect’’ in spin glasses. More sophisticated examples of memory phenomena have recently been reported and illustrated by low-frequency ac susceptibility experiments.^{27–29} In these experiments, the magnetic memories are created by intermittent halts at constant temperatures $T_s < T_g$ of duration t_s during cooling from above T_g . A halt at constant temperature allows the system to relax towards its equilibrium state at T_s , causing a decay of the magnitude of both components of the low-frequency ac-susceptibility. This equilibrated state becomes frozen in on further lowering the temperature, and can be retrieved on reheating. A most intriguing fact in these experiments is that equilibration at one high temperature has no influence on the behavior only a few kelvin below (outside a region of overlap). That is, if a second halt is made at a lower temperature T'_s , an independent aging process occurs, that appears indistinguishable from the aging process observed on cooling without a stop at the higher temperature. This indicates that the equilibrium states at the two temperatures are different or chaotic. However, in spite of an obvious reconfiguration of the spin structure at T'_s , there is a full memory of the original equilibration at T_s when this temperature is recovered on heating. (The weak low-frequency ac field employed in this kind of experiment does not affect the nonequilibrium processes that are intrinsic to the sample, but works only as a nonperturbing probe of the system).

To further illustrate the memory behavior and the aging phenomenon, we show in Fig. 5(a) results on the temperature dependence of the remanent magnetization. The thermo-remanent (TRM) and isothermal remanent (IRM) are measured on heating the sample in zero field from a low temperature. The different curves have been measured after cooling the sample using a protocol described below:

(1) The sample is cooled in constant field H_o (TRM) or zero field (IRM) from a reference temperature above T_g to a stop temperature T_s , where the sample is kept a stop time t_{s1} without changing the field.

(2) A field change is made: In the TRM case the field is either cut to zero (zero-field stop, ZFS) or kept constant (field stop, FS); for the IRM, H_o is applied. The new magnetic field value is kept during a time t_{s2} .

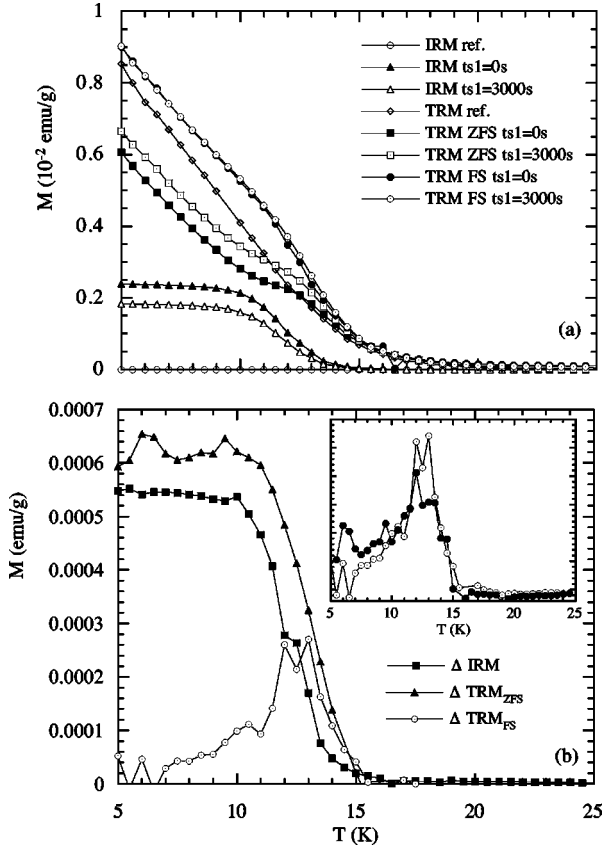


FIG. 5. (a) The remanent magnetization vs temperature measured using a cooling protocol as described in the main text. $T_s = 11$ K, $H_o = 20$ Oe. (b) The difference between the pairs of curves shown in (a): Δ IRM, Δ TRM_{ZFS}, and Δ TRM_{FS}. The inset shows the difference (Δ TRM_{ZFS} - Δ IRM) and Δ TRM_{FS} (which is marked by the same symbols as in the main frame).

(3) The field is then switched back to its initial value and the sample is immediately cooled to a lowest temperature T_{min} , where

(4) the field is cut to zero (TRM) [or kept at zero (IRM)] and the remanent magnetization $M_{TRM}(T)$ (denoted as TRM_{ZFS} and TRM_{FS} for the case of ZFS and FS, respectively) or $M_{IRM}(T)$ (denoted as IRM) is measured on heating the sample at a constant heating rate.

Figure 5(a) shows two different TRM_{ZFS} curves, two TRM_{FS} curves, and two IRM curves all using $T_s = 11$ K. The different curves are measured for two different values of t_{s1} : 0 s and 3000 s, respectively, and in all cases $t_{s2} = 3000$ s. There are also two reference curves plotted in the figure. One ordinary TRM curve, i.e., the sample is directly cooled to $T_{min} = 5$ K, where the field is switched off and the remanent magnetization is recorded on heating. The other is the zero-field reference curve which is measured after cooling in nominal zero field and recording the magnetization on reheating in the same nominal zero field.

There is a significant difference between the remanent magnetization curves in Fig. 5(a) measured using different stop times, t_{s1} in constant field. During the stop at constant temperature T_s , the system ages and the response to a field change during t_{s2} alters, (c.f. Fig. 3). A longer wait time gives a smaller change of the magnetization. When the field is recovered an unperturbed response is maintained during

about 1 s, then the cooling is recaptured and a part of the excess magnetization lost or gained during t_{s2} is frozen in. Looking again at the curves in Fig. 5(a) and comparing the $t_{s1} = 0$ s to the $t_{s1} = 3000$ s, we see that the 0 s curve lies significantly below the 3000 s curve for TRM_{ZFS} whereas the 0 s curve lies above the 3000 s curve for IRM. This effectively illustrates the influence of aging on the magnetic relaxation of our system. Looking at the TRM_{FS} curves and comparing these to the reference TRM, we see that the two TRM_{FS} curves lie significantly above the reference curve, i.e., there has been a considerable reinforcement of the spin structure during the total stop time $t_{s1} + t_{s2}$ at constant field and temperature. (Although there is a small downward relaxation of the FC magnetization during the stop at 11 K, the dominating influence of the equilibration process at T_s is to reinforce the spin structure causing a slower decay of the TRM when passing through T_s .) On the other hand, the difference between stopping 3000 and 6000 s at T_s is significant but comparably smaller. Looking at the overall behavior, the IRM remanence disappears rapidly when the temperature increases above T_s . The TRM_{ZFS} and TRM_{FS} curves similarly coalesce at a temperature somewhat above T_s , but remain finite up to a temperature slightly above T_g . (There is also a weak tail in the TRM curves up to a temperature a few degrees higher than T_g that may indicate a marginal influence of Sr-ion inhomogeneity in the sample.)

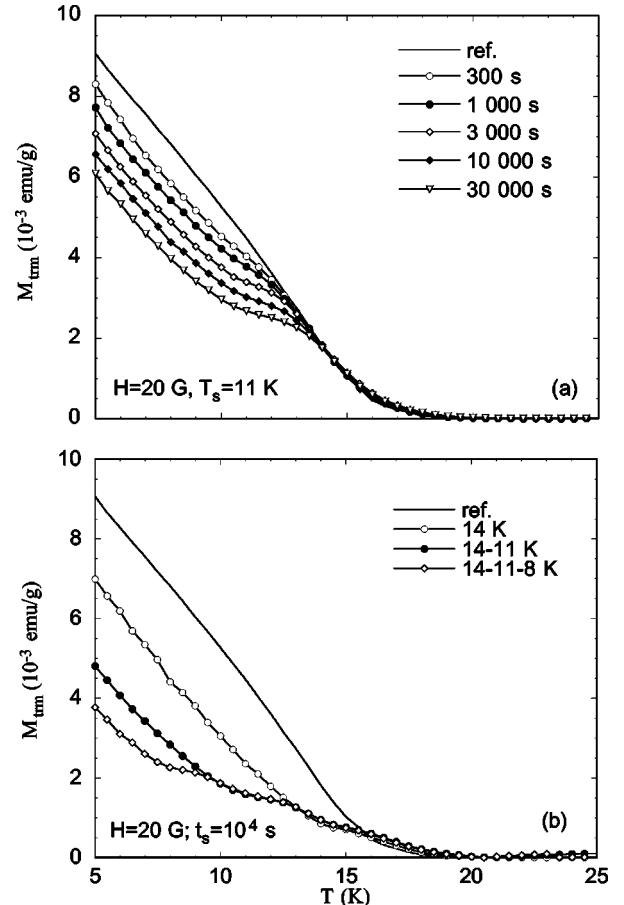


FIG. 6. (a) TRM_{ZFS} vs temperature using different values of t_s as indicated in the figure. (b) TRM_{ZFS} vs temperature halting at 14, 11, and 8 K; 14 and 11 K; 14 K and a reference curve without a halt. The stop times at each halt are equivalent, $t_s = 10^4$ s.

Provided the experiments are made at low enough field, where there is a linear response to a field change and one can relate the results from different relaxation experiments through the principle of superposition. This implies, e.g., that³⁰

$$M_{\text{ZFC}}(t_w, t) = M_{\text{FC}}(0, t_w + t) - M_{\text{TRM}}(t_w, t).$$

Figure 5(b) shows the difference plots of the TRM_{ZFS} and IRM curves shown in Fig. 5(a) giving a direct measure of the frozen-in excess magnetization due to aging. Also plotted in the figure is a difference plot of the TRM_{FS} curves. The inset shows a plot of $\Delta\text{TRM}_{\text{ZFS}} - \Delta\text{IRM}$ and $\Delta\text{TRM}_{\text{FS}}$, the two curves look very similar and suggest an increased validity of the superposition principle to apply also to the temperature dependence of the frozen-in excess magnetization of a spin glass. (ΔIRM reflects M_{ZFC} , $\Delta\text{TRM}_{\text{ZFS}}$ reflects M_{TRM} , and M_{FC} corresponds to $\Delta\text{TRM}_{\text{FS}}$.)

To further illustrate the possibility to usefully investigate rather complicated dynamic properties by simple M vs T experiments, we show in Fig. 6(a) TRM_{ZFS} curves measured after different halt times t_s at $T_s = 11$ K. (In these experiments, $t_{s1} = 0$ and $t_{s2} \equiv t_s$.) The halt times are logarithmically spaced and the corresponding TRM_{ZFS} curves consequently show almost equidistant separation at low temperatures. The different curves merge with the reference curve at higher and higher temperature with larger values of t_s . Figure 6(b) shows an example of a multiple memory behavior in the spin-glass phase. The figure shows TRM_{ZFS} curves where a sequence of 0, 1, 2, and 3 stops have been made during cooling. Among the curves are also reference ones employing 0, 1, and 2 stops at the same temperatures and for equivalent stop time $t_s = 10^4$ s. All curves merge with the corresponding reference curves just above their lowest common stop temperature. A memory phenomenon similar to this is expected to occur in a system with independent relaxing entities governed by thermally activated relaxation.

It is more surprising that a spin glass in a nonequilibrium and chaotic phase allows such a multiple memory of ‘‘historic’’ dynamic processes. Similar experiments were performed on a canonical AgMn 3D spin glass³¹ to check the validity of the method.

IV. CONCLUSION

We have found that a highly homogeneous $\text{La}_{0.95}\text{Sr}_{0.05}\text{CoO}_3$ has dynamic magnetic properties indistinguishable from those of a 3D spin-glass phase. A dynamic scaling analysis using conventional critical slowing down indicates a finite transition temperature to the spin-glass phase at $T_g \approx 14.6$ K. Long time relaxation and aging effects were observed at all temperatures in the spin-glass phase. Temperature cycling experiments also confirm that $\text{La}_{0.95}\text{Sr}_{0.05}\text{CoO}_3$ has a low-temperature spin-glass phase. The existence of a spin-glass phase evidences disorder and frustration; i.e., there is a random distribution of ferromagnetic and antiferromagnetic interaction in the system.

We have also introduced a simple dc-magnetization method, that is applicable to most commercial magnetometers, to derive rather sophisticated knowledge about the dynamics of complex slowly relaxing magnetic systems.

ACKNOWLEDGMENTS

Financial support from the Swedish Natural Science Research Council (NFR) is acknowledged. This work was also sponsored by the Swedish International Development Agency (Sida), the Swedish Agency for Research Cooperation (SAREC), and the International Science Programs (ISP) of Uppsala University. The authors thank Dr. P. V. Phuc for the x-ray-diffraction measurements and phase analysis and Dr. P. Jönsson for her valuable comments. Special thanks are due to Professor N. Chau, Dr. N. L. Minh, and Dr. B. T. Cong for their help in sample preparation.

- ¹M. Itoh, I. Natori, S. Kubota, and K. Motoya, *J. Phys. Soc. Jpn.* **63**, 1486 (1994); Masayuki Itoh, Ikuomi Natori, Satoshi Kubota, and Kiyochiro Motoya, *J. Magn. Magn. Mater.* **140-144**, 1811 (1995).
- ²D.N.H. Nam, K. Jonason, P. Nordblad, N.V. Khiem, and N.X. Phuc, *Phys. Rev. B* **59**, 4189 (1999).
- ³S. Mukherjee, R. Ranganathan, P.S. Anikumar, and P.A. Joy, *Phys. Rev. B* **54**, 9267 (1996).
- ⁴R. Caciuffo, J. Mira, J. Rivas, M.A. Señarís Rodríguez, P.G. Radaelli, F. Carsughi, D. Fiorani, and J.B. Goodenough, *Europhys. Lett.* **45**, 399 (1999).
- ⁵R. Caciuffo, D. Rinaldi, G. Barucca, J. Mira, J. Rivas, M.A. Señarís Rodríguez, P.G. Radaelli, D. Fiorani, and J.B. Goodenough, *Phys. Rev. B* **59**, 1068 (1999).
- ⁶V.G. Sathe, A.V. Pimpale, V. Siruguri, and S.K. Paranjpe, *J. Phys.: Condens. Matter* **8**, 3889 (1996).
- ⁷K. Asai, O. Yokokura, N. Nishimori, H. Chou, J.M. Tranquada, G. Shirane, S. Higuchi, Y. Okajima, and K. Kohn, *Phys. Rev. B* **50**, 3025 (1994).
- ⁸J. Mira, J. Rivas, K. Jonason, P. Nordblad, M.P. Brejjo, and M.A.

- Señarís Rodríguez, *J. Magn. Magn. Mater.* **196-197**, 487 (1999).
- ⁹D. Louca, J.L. Sarrao, J.D. Thompson, H. Röder, and G.H. Kwei, *Phys. Rev. B* **60**, 10 378 (1999).
- ¹⁰J. Magnusson, C. Djurberg, P. Granberg, and P. Nordblad, *Rev. Sci. Instrum.* **68**, 3761 (1997).
- ¹¹L. Sandlund, P. Svedlindh, P. Granberg, P. Nordblad, and L. Lundgren, *J. Appl. Phys.* **64**, 5616 (1988).
- ¹²P.C. Hohenberg and B.I. Halperin, *Rev. Mod. Phys.* **49**, 435 (1977).
- ¹³K. Gunnarsson, P. Svedlindh, P. Nordblad, L. Lundgren, H. Aruga, and A. Ito, *Phys. Rev. Lett.* **61**, 754 (1988); L. Sandlund, P. Granberg, L. Lundgren, P. Nordblad, P. Svedlindh, J.A. Cowen, and G.G. Kenning, *Phys. Rev. B* **40**, 869 (1989); P. Granberg, J. Mattson, P. Nordblad, L. Lundgren, R. Stubi, J. Bass, D.L. Leslie-Pelecky, and J.A. Cowen, *ibid.* **44**, 4410 (1991), and references therein.
- ¹⁴L. Lundgren, P. Svedlindh, P. Nordblad, and O. Beckman, *Phys. Rev. Lett.* **51**, 911 (1983); L. Lundgren, P. Svedlindh, and O. Beckman, *J. Magn. Magn. Mater.* **31-34**, 1349 (1983).
- ¹⁵D.S. Fisher and D.A. Huse, *Phys. Rev. B* **38**, 373 (1988); D.S.

- Fisher and D.A. Huse, *ibid.* **38**, 386 (1988).
- ¹⁶J.-P. Bouchaud, L.F. Cugliandolo, J. Kusch, and M. Mezard, in *Spin-Glasses and Random Fields*, edited by A.P. Young (World Scientific, Singapore, 1997), pp. 161–224, and references therein.
- ¹⁷J.-O. Andersson, J. Mattsson, and P. Svedlindh, *Phys. Rev. B* **46**, 8297 (1992).
- ¹⁸D.N.H. Nam, P. Nordblad, N.V. Khiem, and N.X. Phuc (unpublished).
- ¹⁹D.N.H. Nam, R. Mathieu, P. Nordblad, N.V. Khiem, and N.X. Phuc, *Phys. Rev. B* **62**, 1027 (2000).
- ²⁰D.N.H. Nam, R. Mathieu, P. Nordblad, N.V. Khiem, and N.X. Phuc, cond-mat/0007439 (unpublished).
- ²¹K. Jonason and P. Nordblad, *J. Magn. Magn. Mater.* **177-181**, 95 (1998).
- ²²P. Nordblad, in *Dynamical Properties of Unconventional Magnetic Systems*, edited by A.T. Skjeltorp and D. Sherrington (Kluwer, Dordrecht, 1998) pp. 343–346; P. Nordblad and P. Svedlindh, in *Spin-Glasses and Random Fields* (Ref. 16), pp. 1–27, and references therein.
- ²³K. Jonason and P. Nordblad, *Eur. Phys. J. B* **10**, 23 (1999).
- ²⁴P. Nordblad, K. Gunnarsson, P. Svedlindh, and L. Lundgren, *J. Magn. Magn. Mater.* **71**, 17 (1987); P. Svedlindh, K. Gunnarsson, P. Nordblad, and L. Lundgren, *ibid.* **71**, 22 (1987).
- ²⁵L. Lundgren, P. Nordblad, P. Svedlindh, and O. Beckman, *J. Appl. Phys.* **57**, 1 (1985).
- ²⁶P. Nordblad, P. Svedlindh, L. Lundgren, and O. Beckman, in *Multicritical Phenomena*, edited by R. Pynn (Plenum, New York, 1984); C. Djurberg, J. Mattsson, P. Nordblad, R. Stubi, and J.A. Cowen, *Physica B* **194-196**, 303 (1994).
- ²⁷T. Jonsson, K. Jonason, and P. Nordblad, *Phys. Rev. B* **59**, 9402 (1999).
- ²⁸K. Jonason, E. Vincent, J. Hammann, J.P. Bouchaud, and P. Nordblad, *Phys. Rev. Lett.* **81**, 3243 (1998); C. Djurberg, K. Jonason, and P. Nordblad, *Eur. Phys. J. B* **10**, 15 (1999); K. Jonason, P. Nordblad, E. Vincent, J. Hammann, and J.P. Bouchaud, *ibid.* **13**, 99 (2000).
- ²⁹T. Jonsson, K. Jonason, P. Jönsson, and P. Nordblad, *Phys. Rev. B* **59**, 8770 (1999).
- ³⁰C. Djurberg, J. Mattsson, and P. Nordblad, *Europhys. Lett.* **29**, 163 (1995).
- ³¹R. Mathieu, P. Jönsson, D.N.H. Nam, and P. Nordblad, cond-mat/0007070 (unpublished).